Hindawi
Journal of Sensors
Volume 2019, Article ID 5067081, 15 pages
https://doi.org/10.1155/2019/5067081

Research Article

Parameter Optimization on FNN/PID Compound Controller for a Three-Axis Inertially Stabilized Platform for Aerial Remote Sensing Applications

Xiangyang Zhou,[1] Hao Gao,[1] Yuan Jia,[1] Lingling Li,[1] Libo Zhao,[2] and Ruifang Yu[3]

[1]*School of Instrumentation Science and Opto-Electronics Engineering, Beihang University (BUAA), Beijing 100191, China*
[2]*State Key Laboratory for Manufacturing Systems Engineering, Xi'an Jiaotong University, Xi'an 710049, China*
[3]*Institute of Geophysics, China Earthquake Administration, Beijing 100081, China*

Correspondence should be addressed to Ruifang Yu; yrfang126@126.com

Received 16 April 2018; Revised 31 August 2018; Accepted 27 September 2018; Published 26 March 2019

Guest Editor: Pasquale Imperatore

This paper presents a composite parameter optimization method based on the chaos particle swarm optimization and the back propagation algorithms for a fuzzy neural network/proportion integration differentiation compound controller, which is applied for an aerial inertially stabilized platform for aerial remote sensing applications. Firstly, a compound controller combining both the adaptive fuzzy neural network and traditional PID control methods is developed to deal with the contradiction between the control precision and robustness due to disturbances. Then, on the basis of both the chaos particle swarm optimization and the back propagation compound algorithms, the parameters of the fuzzy neural network/PID compound controller are optimized offline and fine-tuned online, respectively. In this way, the compound controller can achieve good adaptive convergence so as to get high stabilization precision under the multisource dynamic disturbance environment. To verify the method, the simulations are carried out. The results show that the composite parameter optimization method can effectively enhance the convergence of the controller, by which the stabilization precision and disturbance rejection capability of the proposed fuzzy neural network/PID compound controller are improved obviously.

1. Introduction

Aerial remote sensing has an increasing attention in environmental applications: disaster monitoring, intelligent agriculture, pollution detection, etc. Natural disasters appear in characteristics of high frequency and intensity and often result in huge losses in their area of destruction [1]. Therefore, gathering information and continuously monitoring the affected areas are crucial to assess the damage and speed up the recovery process [2]. Remote sensing technologies can take a significant place for decision-makers for the calculation and estimation of the environment impacts [3]. On the other hand, precision agriculture includes various technologies that allow agricultural professionals to use information management tools to optimize agriculture production [4]. The agricultural practices, planting patterns, the stage of growth in the vegetation, soil composition, and humidity are important factors that affect the present-day visibility of buried structures such as crop or soil marks [5]. There are great challenges for accurate predictive mapping at regional scales for an agroecosystem [6]. Remote sensing technologies offer opportunities to break down the silos between energy, water, and resource management through cheaper, automated, and high spatiotemporal resolution data collection. Remote sensing via aerial (i.e., manned or unmanned) vehicles generally allows for more detailed spatial resolution than satellite measurements [7].

Inertial stabilized platform (ISP) is a key component for an aerial remote sensing system, which is mainly used to hold and control the line of sight (LOS) of the imaging sensors keeping steady in an inertial space [8–13]. For a high-resolution aerial remote sensing system, it is crucial to isolate the attitude changes of aircraft in three axes and to reject the multisource disturbances inside or outside of the aircraft body in real time. The first fundamental objective of an ISP is to help the imaging sensors to obtain high-quality images of the target or target region. Therefore, the most critical performance metric for an ISP is the disturbance rejection.

Many different control methods with high accuracy and stability are developed through suppressing various disturbances. In [14], a dual-rate-loop control method based on the disturbance observer (DOB) of angular acceleration is proposed to improve the control accuracy and stabilization of the ISP. In [15], a self-adaptive online genetic algorithm tuning is proposed to optimize the proportion integration differentiation (PID) parameters of the ISP, which improve the system control precision and stability and response speed. In [16], a self-tuning fuzzy/PID control strategy is proposed to improve the dynamic performance of the ISP. In [17], an automatic disturbance rejection controller (ADRC) is proposed to solve the issues such as system model uncertainty and measurement noise in a three-axial ISP control system. In [18], a method combining a Kalman filter and a disturbance observer is put forward to improve the inertial stabilization performance of an aerial photoelectric platform. In [19], a compound control strategy combining the extended disturbance observer (EDO) and continuous robust integral of the sign of error (RISE) is proposed to improve the stability precision of an ISP. In [20], an integrated control method using both feed-forward control and disturbance observer is designed to improve the stabilization precision of the ISP.

As an intelligent control method, the fuzzy control is a non-open-loop control system that is based on fuzzy logic inference. It is especially suitable for the control of nonlinear, time-varying, and delay systems [21]. The control performance of the system depends on the parameter setting, so it is not easy to achieve the desired control effect [22]. Although the PID regulator can get higher steady-state accuracy and dynamic characteristics, the parameter tuning is difficult. The determination of the conventional PID controller parameter tuning is based on obtaining the mathematical model of controlled objects and the rules, which is difficult to adapt to complex control systems [23]. Comparatively, the fuzzy control method is a kind controller of language, which can reflect the approximate optimal control behavior of controller and have strong robustness and stability to adapt to different object controls [24]. Therefore, the method combining both the adaptive fuzzy and the traditional PID control methods should be developed to solve the contradiction between the control precision and robustness on disturbances.

However, the method of fuzzy controller essentially is a nonlinear controller whose control algorithm is based on intuition and experience on the plant; it does not have any automatic learning capabilities to handle the uncertainty. It is well known that the adaptive neural network (NN) control has a learning capability and has been considered as a powerful tool to identify any nonlinear function to any desired accuracy in control and applications for nonlinear systems [25]. Therefore, although it is a particularly difficult problem for the fuzzy system to determine the membership function, the input-output of the NN can approximate any function. So in the fuzzy system design, it can take advantage of the learning ability of the NN and operation by adjusting the weight membership functions in learning [26]. However, the parameters of the existing fuzzy neural network (FNN)/PID controller are large and the initial value has a great influence on the convergence of the controller; it is difficult to find a good initial value of parameters in the practical application to the ISP to get a good control effect. Therefore, it is difficult to obtain more suitable initial values of parameters by the ordinary trial and error method. So it is necessary to investigate the parameter optimization algorithms to obtain better parameters for the system.

The particle swarm optimization (PSO) is a computational intelligence-oriented, stochastic, population-based global optimization technique [27]. It is concerned with the elementary algorithm, which has the characteristics of simplicity, easy implementation, and few parameters to be adjusted [28]. However, the PSO seems to be sensitive to the tuning of its parameters [29]. These advantages lead PSO to be applied broadly to different areas. For the basic PSO, the result easily falls into the local optimum with random initial choice, because of the nonuniform distribution of initial particles, which will weaken the global search ability of the PSO. Once getting trapped in local optimum during the process of optimization, it is very easy to cause all particles to stagnate in the extreme value point [30]. Therefore, when the algorithm runs into prematurity, the random perturbation strategy is adopted for the best individual and the randomly selected individual to help them being out of the local minimum [31]. Since the PSO has the drawback of stopping optimizing when reaching a near-optimal solution [27], the chaos mechanism is proposed to help the PSO to optimize the searching result. Thus, an improved algorithm based on the mechanism of chaos and the PSO, i.e., the chaos particle swarm optimization (CPSO) algorithm, is proposed to adjust the parameters offline. In [32], the chaos searching is proposed for global optimization problems and parameter inversion of the nonlinear sun shadow model, which can improve the computing accuracy and computing efficiency of the global optimization problems. In [33], the chaos is applied to avoid the untimely aggregation of particle swarm and improve the mean best of the algorithm and the success rate of search. In [34], a chaotic searching is applied to improve the global search performance, and the applying results show that the CPSO algorithm is very efficient at solving global optimization problems and is a good approach for reliability analysis. Furthermore, the back propagation (BP) algorithm is used to adjust online to obtain the optimized parameters. In this way, the control system can achieve better control results.

In this paper, to improve the ability of disturbance rejection of an aerial ISP, an FNN/PID compound control scheme is first designed. Then, a composite parameter optimization method based on the CPSO and BP algorithms is proposed

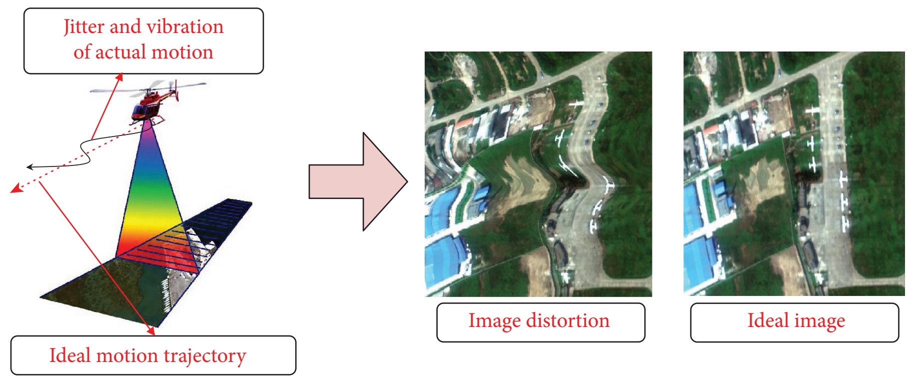

FIGURE 1: Schematic diagram: effect of the ISP on improving the image quality in an aerial remote sensing system for aerial remote sensing applications.

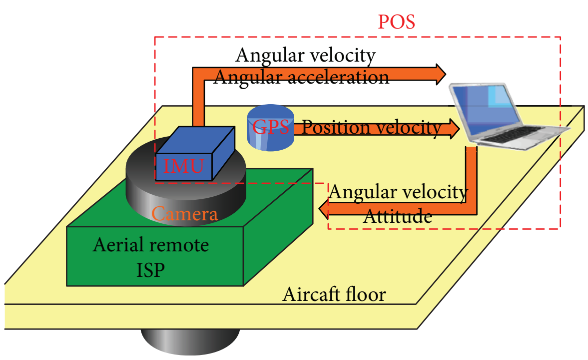

FIGURE 2: Schematic diagram of an aerial remote sensing system [44].

to improve the adaptive convergence performance of the compound controller. To verify the method, the simulations are carried out.

2. Background

2.1. Aerial Remote Sensing System. Figure 1 shows a schematic diagram to illustrate the important effect of the ISP on improving the image quality in an aerial remote sensing system for aerial remote sensing applications. Due to the serious influences caused by disturbances arising from diverse sources, including inside or outside of the aviation platform, it becomes very difficult to keep the LOS steady, particularly for the case of the jitter of three angular attitudes of an aircraft. Thus, the case of unideal images replacing the ideal images will occur. So the high-precision ISP, which is typically mounted on a movable platform, is indispensable to isolate disturbances derived from diverse sources [9, 12].

Figure 2 shows the schematic diagram of an aerial remote sensing system. Generally, an aerial remote sensing system consists of four main components: a three-axis ISP, a remote sensing sensor, a position and orientation system (POS), and an aviation platform. When the aviation platform rotates or jitters, the control system of three-axis ISP gets the high-precision attitude reference information measured by the POS and then routinely controls the LOS of the imaging sensor to achieve accurate pointing and stabilizing relative to ground level and flight track. The POS, which is mainly composed of the inertial measurement unit (IMU), the GPS receiving antenna, and the data processing system, is used to measure the minor angular movement of the imaging sensor.

2.2. Operating Principle of Three-Axis ISP System. Figure 3 shows the schematic diagram of the three-axis ISP's principle. We can see that the ISP consists of three gimbals, which are azimuth gimbal (A-gimbal), pitch gimbal (P-gimbal), and roll gimbal (R-gimbal). Among them, the A-gimbal is assembled on the P-gimbal and can rotate around the Z_a axis. Likewise, the P-gimbal is assembled on the R-gimbal and can rotate around the X_p axis. The R-gimbal is assembled on the basement and can rotate around the Y_r axis.

From Figure 3, we can see the relationships between the three gimbals: G_p, G_r, and G_a, respectively, which stand for the rate gyro that measures the inertial angular rate of P-gimbal, R-gimbal, and A-gimbal. E_r, E_p, and E_a, respectively, stand for the photoelectric encoder which measures relative angular between gimbals. M_r, M_p, and M_a, respectively, stand for the gimbal servo motor which drives R-gimbal, P-gimbal, and A-gimbal to keep these three gimbals steady in an inertial space.

2.3. Three Closed-Loop Compound Control Scheme. Figure 4 shows the block diagram of the traditional three-loop control system for ISP. Conventional stabilization techniques employ rate gyros, rate integrating gyros, or rate sensors to sense rate disturbances about the LOS. In Figure 4, the blocks of G-pos, G-spe, and G-cur separately represent the controllers in the position loop, speed loop, and current loop; the PWM block represents the power amplification used for the current amplifier to drive the torque motor; L represents the inductance of a torque motor, and R represents the resistance; K_t represents the torque coefficient of the motor, and N is the transition ratio from the torque motor to the gimbals; J_m represents the moment of inertia

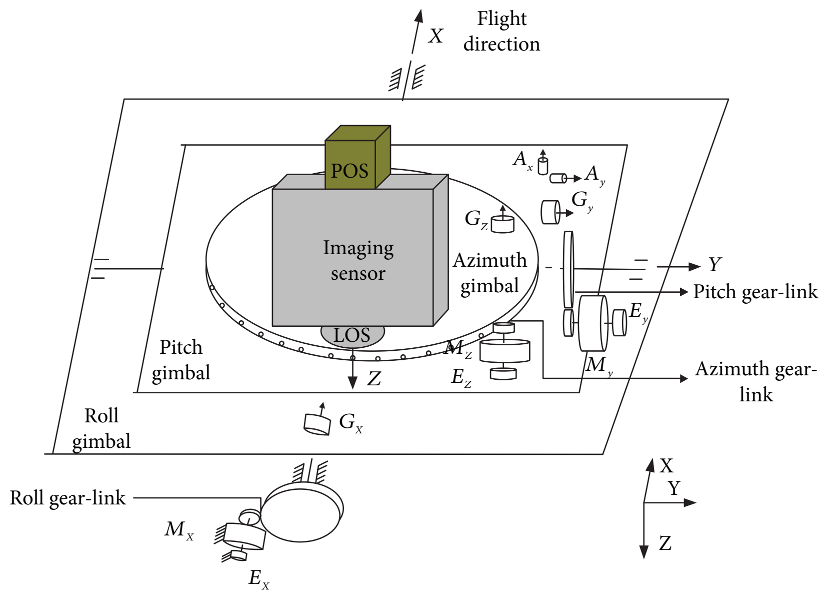

FIGURE 3: Schematic diagram of the three-axis ISP's principle.

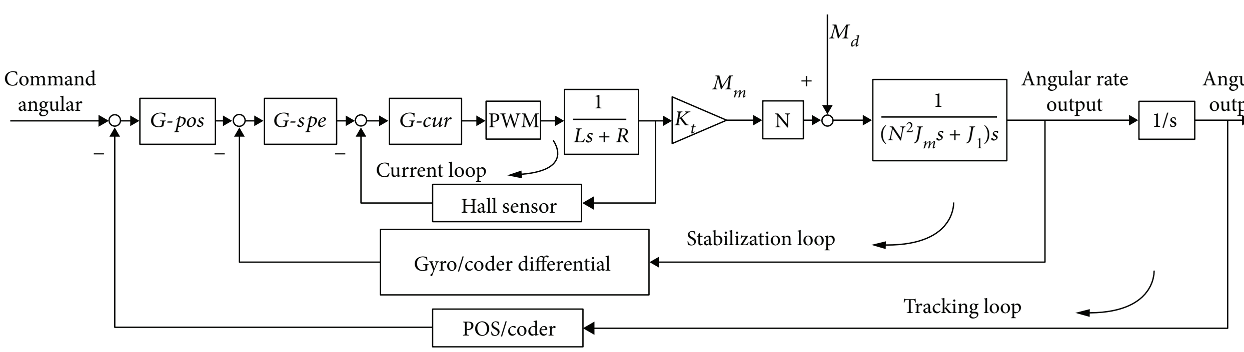

FIGURE 4: A block diagram of traditional three-loop control system for ISP [44].

of the motor, and J_l represents the moment of inertia of the gimbals along the rotation axis.

3. Design of the FNN/PID Compound Controller

In the FNN/PID control method, the input interface has two nodes, i.e., the error (e) and change of the error (ec), respectively. The role of the fuzzification layer is to make the input of a reasonable fuzzy segmentation, in which the number of nodes is equal to the number of variables [29]:

$$f_1(i) = X = [x_1, \ldots, x_n], \quad n = 2, \tag{1}$$

where X stands for the domain.

When the method is applied to the ISP, the fuzzy language of each input variable is divided into seven segments. According to the working principle of the ISP, different Gauss functions and bell functions are used to represent the different fuzzy subsets which are expressed as follows:

$$f_{;2}(i,j) = \mu_{\mathrm{Aij}} = \exp\left[\frac{-\left(X_i - c_{ij}\right)^2}{\sigma_{ij}^2}\right], \quad i = 1, 2, j = 2, 3, 4, 5, 6, \tag{2}$$

$$f(i,j) = \mu_{\mathrm{Aij}} = \frac{1}{\left(1 + \left|\left(X_i - c_{ij}\right)/a_{ij}\right|\right)^{2\sigma_{ij}^2}}, \quad i = 1, 2, j = 1, 7, \tag{3}$$

where X_i stands for the input variable; c and σ stand for the activation function centers and widths, respectively; and a stands for the fuzzy subsets corresponding to fuzzy variables. For the different fuzzy subsets, the different membership functions should be chosen. In (2), i.e., the Gaussian function's marginal value and middle value are close to 0 and 1, respectively, which is suitable for the fuzzy subset with a large membership degree of intermediate element. In (3), i.e., the bell function's marginal value is close to 1, which is suitable for the fuzzy subset with a large membership degree of the boundary element [35].

Different from the general FNN/PID control algorithm that sets up a relatively simple activation function, the improved methods of membership function parameters are diverse from each other. This control method absorbs the experience of fuzzy/PID control in the membership function design. Therefore, it is more suitable for the system characteristics of the ISP, and its parameters are no longer updated and adjusted in the BP algorithm. Thus, the blindness of parameter updating is avoided, which further results in a short computing time and a good control effect.

Corresponding to the ISP system, the number of the nodes of the fuzzy rule layer is 49, and the method of fuzzy inference is as follows [36]:

$$\begin{aligned} f_3(j) &= \prod_{j=1}^{N} f_2(i,j) = \mu_{A1k}(x_1) * \mu_{A2k}(x_2), \\ N &= \prod_{i=1}^{n} N_i, \end{aligned} \tag{4}$$

where k is the number of fuzzy rules.

For the output layer, it can be obtained by the output of the upper layer and the connection weight, as shown as follows [32]:

$$f_4(j) = w \cdot f_3 = \sum_{j=1}^{N} w(i,j) \cdot f_3(j), \tag{5}$$

where w stands for the connection weight matrix.

The output of the improved FNN/PID controller is used as the compensation of the constant PID parameters, as shown as

$$\begin{aligned} K_p &= K_{p0} + \mathrm{FNN}\left(\Delta K_p\right), \\ K_i &= K_{i0} + \mathrm{FNN}(\Delta K_i), \\ K_d &= K_{d0} + \mathrm{FNN}(\Delta K_d), \end{aligned} \tag{6}$$

where K_{p0}, K_{i0}, and K_{d0} represent the initial parameters of the fuzzy/PID controller and $\mathrm{FNN}(\Delta K_p)$, $\mathrm{FNN}(\Delta K_i)$, and $\mathrm{FNN}(\Delta K_d)$ represent the outputs of the improved FNN/PID controller.

So the output of the controller is expressed as follows:

$$\mathrm{u}(k) == k_p[e(k) - e(k-1)] + k_i \sum_{i=1}^{k} e(i) + k_d[e(k) - e(k-1)]. \tag{7}$$

The improved FNN/PID controller controls the ISP by adding the PID value of real-time adjustment and the fixed PID value. In this case, the FNN can only deal with the small change which reduces the dependence on the initial value and makes the adjustment time shorter. Because the whole system is not entirely dependent on the output value of the adaptive adjustment part, it can guarantee the stability and avoid the divergence.

The improved FNN/PID controller only needs to determine the weights of the controller, since it uses fuzzy/PID controller's fuzzy subset number, membership function, quantization factor, and constant PID parameter value. Since the output of the method is small, the effect of the initial value of the weight coefficient on its output is limited. Thus, the superior control effect can be obtained by only the randomly obtained parameters. Figure 5 shows the schematic diagram of the FNN/PID compound controller structure.

4. Composite Parameter Optimization Based on CPSO and BP Algorithms

The FNN/PID controller inherits the advantages of fuzzy control in acquiring knowledge, which has the ability of the neural network to approach any nonlinear function at the same time. However, the parameters of this method are large and the initial value has a great influence on the convergence of the controller; it is difficult to find a good initial value of parameters in the practical application for the ISP to get a good control effect. The general FNN/PID controller is difficult choosing the initial value which influences the improvement of the control accuracy and the convergence.

If the control level of the FNN/PID controller is expected to improve, configuring a series of parameters which are more appropriate is necessary. Thus, the parameter optimization problem is the key to the control effect of the controller. The structure of the controller is a forward neural network, which can adapt to the control request of the controlled object by adjusting the weight of the network itself. At the initialization stage of the algorithm, the position of the particle is initialized by chaos. The weight coefficients are encoded as vectors and expressed as Para. The number of particle swarm optimization is selected as N. Chaos initialization is applied to randomly produce n-dimensional vectors $z_1 = (z_{11}, z_{12}, \cdots, z_{1n})$, which is formed from $z_{i+1j} = \mu z_{ij}(1 - z_{ij})(j = 1, 2, \cdots, n, i = 1, 2, \cdots, N-1)$and carried to the range of optimized variable $x_{ij} = a_j + (b_j - a_j) z_{ij}(j = 1, 2, \cdots, n, i = 1, 2, \cdots, N-1)$ as the position of initialized particle swarm. In addition, the other system parameters, including acceleration constants, the maximum inertia weight, and the minimum inertia weight, are assigned to the numerical value based on other academic papers, in which the values of c_1, c_2, $w_{p\,\max}$, and $w_{p\,\min}$ are 2, 2, 1.2, and 0.4, respectively.

4.1. Particle Swarm Optimization Algorithm (PSO). If the neural network is used as the controller in the control system, the astringency of the training algorithm depends largely on the choice of the initial weights of the network and the general approach is cut-and-trial. However, it is difficult to achieve for complex problems. It will directly lead to the poor parameter setting for the controller and poor control quality. Therefore, it is very important to optimize the weights of the network by using the optimization algorithm. For the offline optimization of the controller parameters, an improved

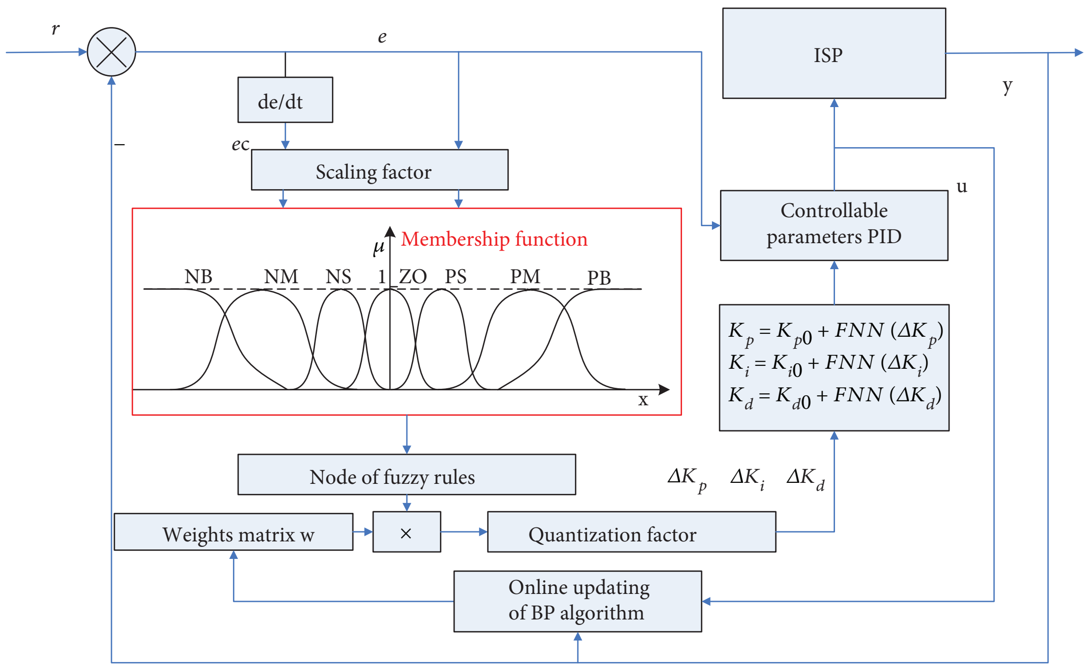

FIGURE 5: Schematic diagram of the FNN/PID compound controller structure.

algorithm based on the mechanism of chaos and the PSO, i.e., the CPSO, is proposed.

The PSO adopts the velocity-position model and sets the reasonable inertia weight to balance the global and local search to make the algorithm easier to converge to the optimal or optimal solution. The standard PSO algorithm formulas are shown as (8) [26].

$$\begin{aligned} V_i &= w_p * V_i + c_1 * \text{rand}\ () * (\text{pbest} - \text{Pos}_i) \\ &\quad + c_2 * \text{rand}\ () * (\text{gbest} - \text{Pos}_i), \\ \text{Pos} &= \text{Pos}_i + V_i, \end{aligned} \tag{8}$$

where $i = 1, 2, \dots, n$; n stands for the total number of particles in the population; V_i stands for the moving rate; w_p stands for the inertia weight whose range of value usually is 0.4~1.2; Pos_i stands for the position of the particle; pbest is the location of the best solution in iteration; gbest stands for the location of global best solution; rand () stands for a random number between 0 and 1; and c_1 and c_2 stand for the acceleration constants. The values of c_1 and c_2 are 2, which are determined on the basis of the existing research [37]. The position and velocity of a particle in an n-dimensional space can be expressed as $\text{Pos}_i = (\text{Pos}_1, \text{Pos}_2, \cdots, \text{Pos}_N)$ and $V_i = (v_1, v_2, \cdots, v_N)$, respectively. The fitness function is calculated by the method of self-defined objective function. The fitness value of each particle in each iteration is calculated according to the demand. The optimal value of each particle which is searched by itself currently, and the optimal value in the current population should be stored for dynamically adjusting as experience. According to the characteristics of the determining effect of the system, the fitness function associated with the time is required. So the integral of the absolute value of error multiply time is adopted as the criterion which is also called the ITAE index. The system can obtain the advantages such as fast, smooth, and small overshoot under the ITAE index. Its expression is as follows:

$$J = \int_0^t t|e(t)|dt. \tag{9}$$

The inertia weight is generally linear decreasing weight algorithm as shown in the following formula:

$$w_p(\text{iter}) = w_{p\ \max} - \frac{w_{p\ \max} - w_{p\ \min}}{\text{Iter max} * \text{iter}}, \tag{10}$$

where Iter max stands for the largest evolutionary algebra, iter stands for the algebra, $w_{p\ \max}$ and $w_{p\ \min}$ stands for the maximum inertia weight and the minimum inertia weight, respectively. The introduction of w_p significantly improves the performance of the PSO algorithm such as adjusting the search ability of particles in global and local. Also, the introduction of w_p offsets the problem of the standard PSO algorithm and makes it apply to more practical problems [31]. Figure 6 illustrates the overall view of particle swarm optimization.

In accordance with the above algorithm, the particle continuously updates its velocity and position in the preset solution space and ultimately converges to a suboptimal or optimal location.

4.2. Offline Tuning Based on the CPSO. The chaos is a universal phenomenon in a nonlinear system. The chaos phenomenon has stochastic property, ergodicity, and regularity. In the optimization area, the ergodic property can be used as an optimization mechanism to escape from local optimums. The chaos has been a kind of novel global optimization technique. People pay much attention to the research of the

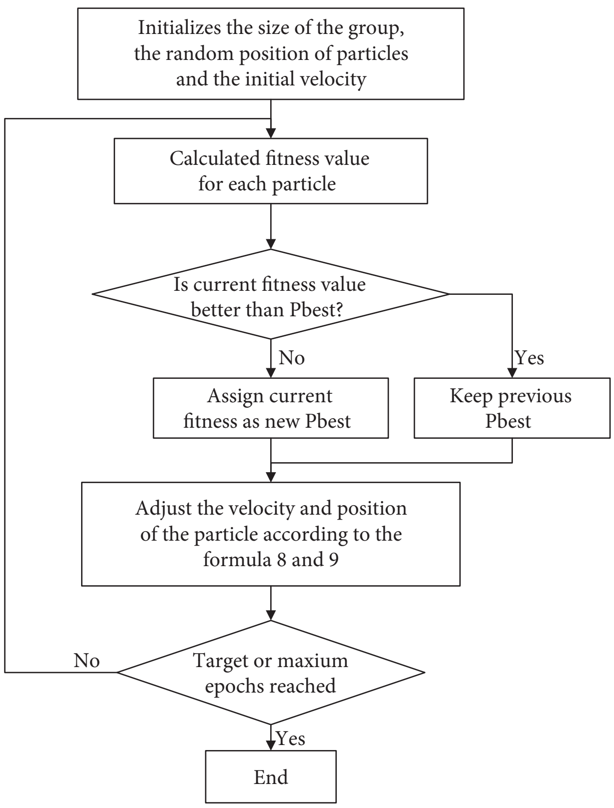

Figure 6: Overall view of particle swarm optimization.

optimization method based on the chaotic search [29, 31, 36, 38]. At present, some scholars have applied it to the optimization of neural network weights and achieved good results.

Based on the three inherent properties of the chaos, including stochastic property, ergodicity, and regularity [39], the new superior individuals are reproduced by chaotic searching on the current global best individuals. For the regularity and ergodicity property, the chaos searching can traverse all states without repeating within a certain range. For the stochastic property applied to selection of individual, a stochastic selected individual from the current population is replaced by the new superior individual. The particle swarm optimization-embedded chaotic search quickens the evolution process and improves the abilities to seek the global excellent result and convergence speed and accuracy.

The chaotic motion is usually generated by a logistic map which is illustrated as follows:

$$\begin{aligned} X_c(n+1) &= \mu X_c(n)[1 - X_c(n)], \\ & n = 0, 1, 2, \ldots, M(0 < X_c(0) < 1), \end{aligned} \tag{11}$$

where μ stands for the control parameter whose range of value is (0, 4). The value of the chaotic control parameter μ is larger, the chaotic degree is higher, and the population structure has suffered more destructive. In the running process of the CPSO algorithm, the control parameters should be dynamically reduced or increased on the basis of the convergence of the population, which can reduce the structural damage to the population and help population escape from local optimizations. In engineering applications and academic studies of CPSO, the value range of the chaotic control parameter μ is usually from 0 to 4 [40]. The chaotic motion is very sensitive to the initial value selection, and the different initial values will be different.

The basic principle of the CPSO algorithm is that chaos initialization is adopted to improve individual quality and chaos perturbation is utilized to avoid the search being trapped in local optimum [31]. The process of the CPSO is conducted as follows:

Step 1. Encode the optimized parameter. The weight coefficients are encoded as vectors and expressed as Para. The number of particle swarm optimization is selected as N. Randomly produce n-dimensional vectors as $z_1 = (z_{11}, z_{12}, \cdots, z_{1n})$. Initialize the particle's position with logistic chaos mapping as $x_{ij} = a_j + (b_j - a_j)z_{ij}$ $(j = 1, 2, \cdots, n, i = 1, 2, \cdots, N - 1)$ which is formed from $z_{i+1j} = \mu z_{ij}(1 - z_{ij})$ $(j = 1, 2, \cdots, n, i = 1, 2, \cdots, N - 1)$ which is carried to the range of optimized variable.

Step 2. Initialize the system parameters, including $c_1 = c_2 = 2$, $w_{p\ \max} = 1.2$, and $w_{p\ \min} = 0.4$.

Step 3. In chaos-aided search, this paper sets appropriate iteration times λ_{co} and small value ξ_{co} as triggers for sharp tuning of chaos. When the CPSO search accuracy is less than ξ_{co} in the λ_{co} iterations, save the current parameter to P_{now}, and assign it to the initial value of the chaotic search P_0, $P_0 = P_{now}$. Randomly initialize the chaotic variable E in the range of (0,0.5) (the logistic map is symmetric in the range of (0,1), and the dimension is consistent with P_{now}. Define $i = 0$. Use the following two equations to generate new parameter values [30]:

$$\begin{aligned} P_0(i+1) &= P_0(i) + \alpha_{co}[2X_c(i) - 1], \\ X_c(i+1) &= 4X_c(i)[1 - X_c(i)], \quad i = i + 1, \end{aligned} \tag{12}$$

where α_{co} is the search radius and the system can traverse the search in a larger range by adjusting the value of α_{co}. However, it is more time-consuming. Through this step, it is expected that the particle velocity and particle position have a proper update value. So the role of α_{co} is only sharp tuning and generally takes smaller values. If a better value is obtained which can be saved as P_b, otherwise, α_{co} should be adjusted.

Chaos phenomena widely existing in nonlinear systems have stochastic property, ergodicity, and regularity, which are widely applied in chaotic search to obtain optimized solution [41]. Chaos has also been used to optimize the weight of a neural network. The chaotic motion is mainly generated by the logistic map. The traversal trajectory is directly affected by the initial value. A slightly different initial value will directly cause the variations of the traversal trajectory. Therefore, the appropriate initial value

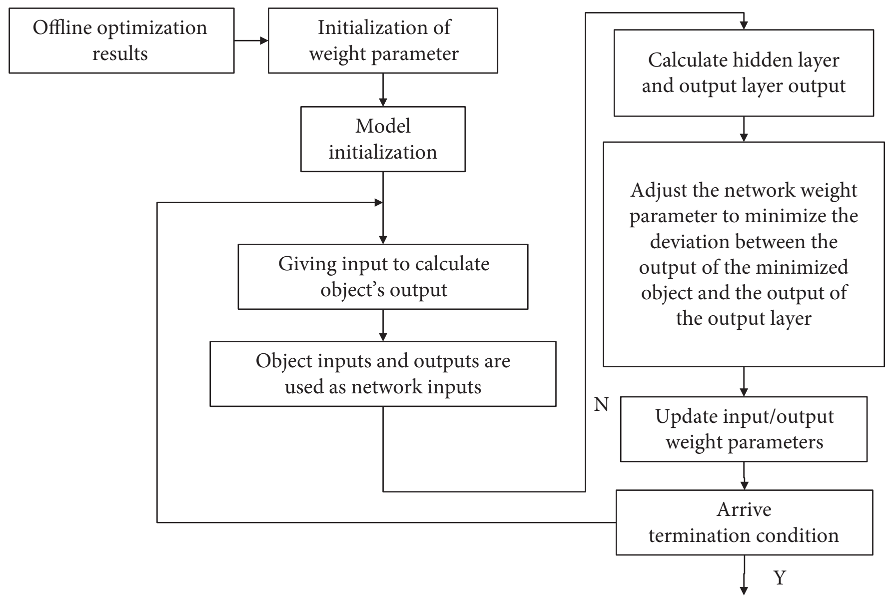

FIGURE 7: Flowchart of online adjustment of the BP algorithm.

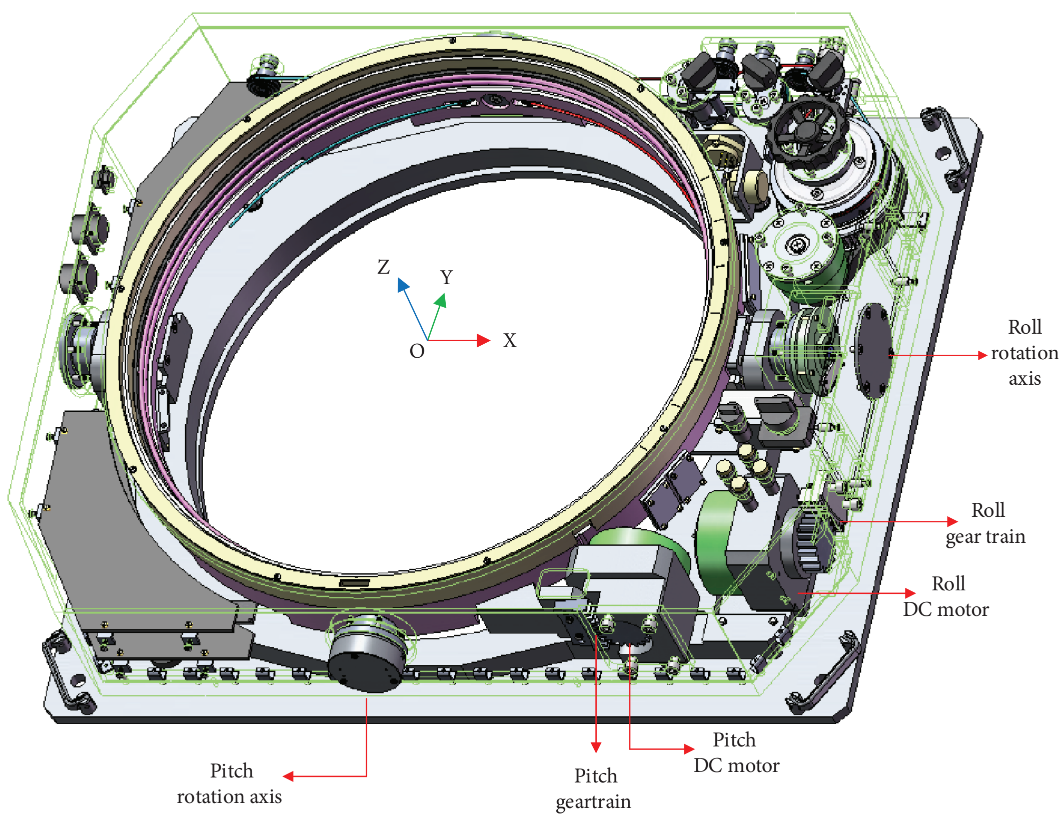

FIGURE 8: Three-dimensional CAD model for a three-axis ISP and its gimbal-transmission system.

of initial parameters has a significant impact on the reduce time-consuming. So we have chosen the appropriate initial value for relevant parameters and initialized the position of the particle by chaos before running the fuzzy neural network/PID compound algorithm. In this way, a PC computer can meet the computation.

Step 4. The chaos strategy is enlargement as the end of the PSO algorithm. In the early stage of search, PSO tends to converge faster, but in the later stage, it is easy to be trapped by local optimizations. Chaos could escape from local optimizations and approach the global optimizations. In the CPSO algorithm, the chaotic method is applied to

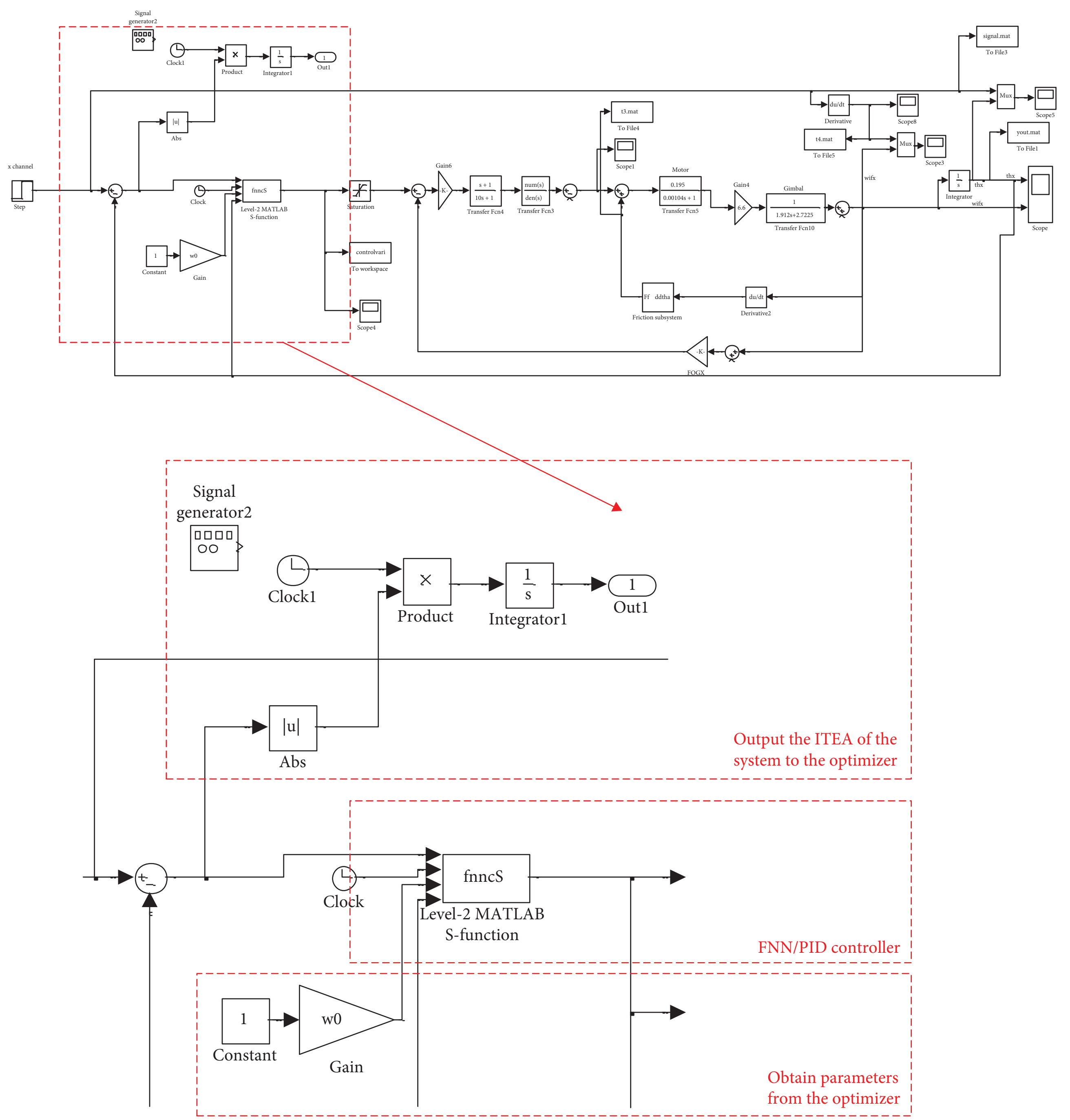

FIGURE 9: Simulink simulation diagram of the CPSO offline for the FNN/PID compound controller.

randomly generate particles in the initialization stage. Based on the standard PSO, the chaotic search strategy is applied in two stages, which assists the PSO in searching optimizations in the first stage, extends their search scopes at the beginning of the second stage, and avoids getting into local optimizations, escape from local optimizations, and approach the global optimizations at end of second stage [42]. The chaos optimization is very time-consuming, and if it is applied in a large scale, so the last step is auxiliary in the global scope. This step is the real search. With the aid of chaos, the CPSO searches for a set of parameter values which are denoted as P_f. Use the following two equations to optimize again:

$$\begin{aligned} P_f(i+1) &= P_f(i) + \beta_{\text{co}}[2X_c(i) - 1], \\ X_c(i+1) &= 4X_c(i)[1 - X_c(i)], \quad i = i+1. \end{aligned} \tag{13}$$

Traverse smaller range with β_{co} as search radius, and the higher value is used as the final parameter of the controller

Table 1: Chosen parameters for the model.

Parameter name	Parameter symbol	Value
The error input interface in FNN/PID control method	e	[−48, 48]
The error change of input interface in FNN/PID control method	ec	[−4, 4]
The scaling factors of the fuzzy/PID controller	K_{p0}, K_{i0}, K_{d0}	1, 0.005, 0.05
Chaotic control parameter	μ	[0, 4]
Acceleration constants	c_1, c_2	2
Inertia weight	w_p	[0.4, 1.2]
Iteration times	λ_{co}	100

saved as P_{final}. If the accuracy is up to standard, the optimization is over. Otherwise, parameters should be recalculated by adjusting β_{co}.

λ_{co} can refer to the total number of iterations of the CPSO algorithm. Its interval does not need to be too dense for designing to assist particles out of the local small. ξ_{co} generally refers to smaller values of the fitness function in the possible range. When the fitness value is difficult to be better, the particles can be adjusted by chaotic motion in order to obtain new searching ability. α_{co} and β_{co} play an important role in supporting and should ensure that the results do not exceed the solution space of the optimization variables in order to avoid waste of computing resources. At the same time, the value of them should be ensured small to guarantee the chaos optimization is kept in a small range.

4.3. Online Tuning Based on the BP Algorithm. The BP algorithm is used to adjust the online simulation when the parameters of the offline suboptimal controller are obtained. The results of offline are close to the optimal values, because of the BP algorithm which is adjusted on the basis of the initial parameters. Therefore, it is necessary to obtain better initial suboptimal parameters in order to ensure real-time online adjustment. The online BP algorithm adjustment is adjusted according to the following formulas [38]:

$$\begin{aligned} c(n+1) &= c(n) + \text{xite} * \frac{\partial E}{\partial c} + \eta * \Delta c(n), \\ \sigma(n+1) &= \sigma(n) + \text{xite} * \frac{\partial E}{\partial \sigma} + \eta * \Delta \sigma(n), \\ w_{\text{all}}(n+1) &= w_{\text{all}}(n) + \text{xite}^* \frac{\partial E}{\partial w_{\text{all}}} + \eta^* \Delta w_{\text{all}}(n), \end{aligned} \tag{14}$$

where w_{all} is the weight matrix of the BP network; xite and η stand for learning factor and momentum factor, respectively; and E stands for the mean squared error (MSE) calculated with the function as $E = (1/2)((\text{rin}(k) - \text{yout}(k))^2$ [43]. The processing is shown in Figure 7.

5. Simulation Model

Figure 8 shows the three-dimensional CAD model for a three-axis ISP and its gimbal transmission system. Figure 9 shows the simulation diagram of the CPSO offline for the FNN/PID compound controller. The simulation model is built to simulate the whole ISP system under friction disturbance which represents the effect of the main disturbance on control precision. When the PSO and the CPSO are used to optimize the initial value of the weight coefficient offline, the optimization program should be written in the file as the optimizer. The controller outputs the parameters to the block diagram with the program to constantly update the value of w_0. It also outputs the value of time multiplied by the integral of the error absolute value to the optimizer. The controller determines the control effect and then calculates the optimization algorithm. In addition, all chosen parameters for the model have been gathered in Table 1 for quick and easy reference.

6. Results and Analysis

6.1. FNN/PID Controller Based on the CPSO. In this paper, the RMS is the abbreviation of the “root mean square” error of the angles in a period of time, which is an error result, calculated from the angle values shown in Figure 10. In Figures 11 and 12, the horizontal axis represents the iteration times in the optimization process that are dimensionless, and the vertical axis represents the fitness values which are the effect of parameter optimization that are also dimensionless.

As it is seen in Figure 10, after the initial value of the weight coefficient of the FNN/PID controller is optimized by the CPSO algorithm, step response overcomes the oscillation problem held by the trial and error method. The overshoot in the CPSO method is reduced from 1.3° RMS to 0.07° RMS with a great decline extent of 94.62%. However, the stability of the system is decreased somewhat which is vibrated in a small error range of 0–0.01° RMS. For the whole range, the RMS error between 0 and 30 seconds is 0.1453° RMS.

As shown in Figure 11, the optimum individual fitness is larger at the previous stage which proves that the control method is not easy to converge. In addition, the change of the optimum individual fitness is small at the end of the iteration whose optimal value at the end of the iteration is 0.5718.

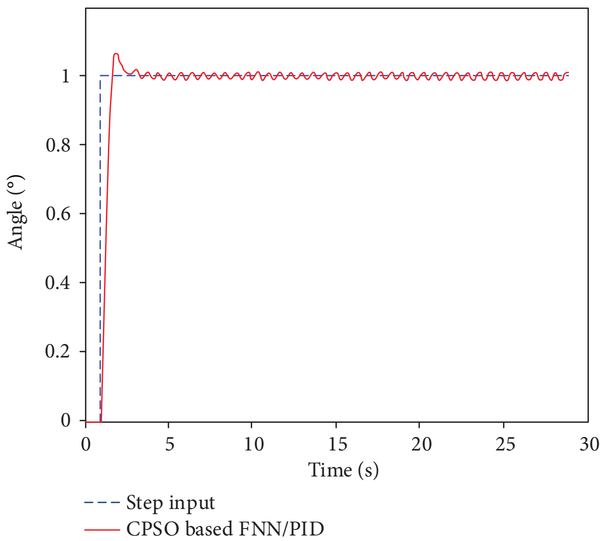

Figure 10: Step response of the FNN/PID controller.

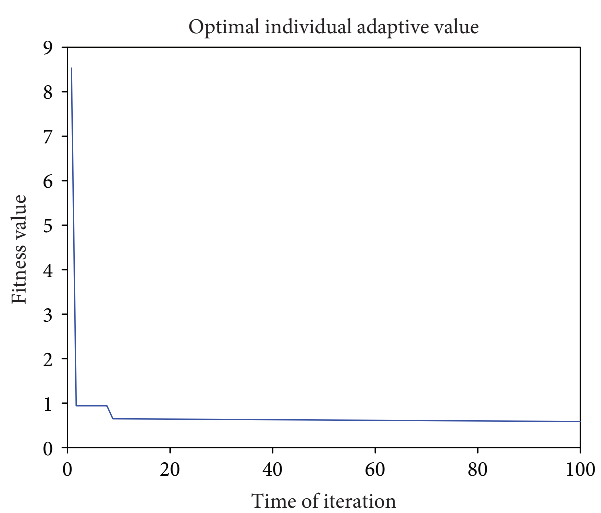

Figure 11: Curves of optimal individual fitness change of optimized particle.

The parameter optimization method improves the performance of the system by traversing all parameters to optimize the parameters. However, it is fundamentally based on the principle of random, and the result can only be guaranteed to be suboptimal. So the method needs further improvement which has not obtained ideal results while using in the ISP. In addition, the optimization algorithm has a long design cycle, and the optimization process is time-consuming. Therefore, it is desirable to design a FNN/PID control method which can achieve a very good control effect without optimization.

6.2. FNN/PID Controller Based on the Composite Parameter Optimization. In this paper, the numerical results on the stabilization precision obtained three different methods, including the proportion integration differentiation (PID), the fuzzy neural network (FNN)/PID compound controller based on trial and error method, and the FFN/PID based on chaos particle swarm optimization (CPSO) and the back propagation (BP) algorithms, responding to the step input, are compared together. Compared with the PID, from 0 s to 30 s, the error of the stabilization precision of the FFN/PID based on the trial and error method is 0.0432°, which is decreased up to 53.6% than that of the PID (which is 0.0931°). The errors of the stabilization precision of the FFN/PID based on CPSO and the BP algorithms are 0.0214°, which is decreased up to 77% than that of the PID. Compared with the FFN/PID based on the trial and error method, the errors of the stabilization precision of the FFN/PID based on CPSO and the BP algorithms have decreased up to 50.5%. From above, it can be concluded that the FNN/PID compound controller can achieve the high stabilization precision with good disturbance rejection ability.-Table 2 shows the numerical results on the stabilization precision obtained by three different methods responded to the step input.

Figure 12(a) shows that the control effect has been considerably improved which demonstrate the effectiveness of the improved FFN/PID approach. And then, the optimal individual fitness in the optimization process is shown in Figure 12(b); the control system is indeed able to find better individual fitness values with the increasing of iterations. In addition, the difference in the magnitude of the fitness values is always small and the variation of optimum fitness is less than 0.0001°. Therefore, it can be shown that the improved FNN/PID control algorithm has less dependence on the initial value of the weight coefficients and is easy to obtain good control results. Based the analysis of theory and simulation, the feedback response times of the speed loop and position loop of FNN/PID control system are 0.617 s and 1.376 s, respectively.

7. Conclusion

In this paper, to improve the convergence of the fuzzy neural network (FNN)/proportion integration differentiation (PID) compound controller applied for an aerial inertially stabilized platform, a composite parameter optimization method is proposed. Based on both the chaos particle swarm optimization (CPSO) and the back propagation (BP) algorithms, the controller parameters are optimized offline and fine-tuned online together. In this way, the FNN/PID compound controller can realize excellent adaptive convergence so as to high stabilization precision under multisource dynamic disturbances. To verify the method, the simulations are carried out. The main conclusions are as follows:

(1) The results show that depending on the proposed composite parameter optimization method, the FNN/PID compound controller can reach good ability in self-learning and self-adaptation, by which the high stabilization precision with good disturbance rejection ability is achieved

(2) Compared with the PID, the FFN/PID methods have excellent stabilization precision and the

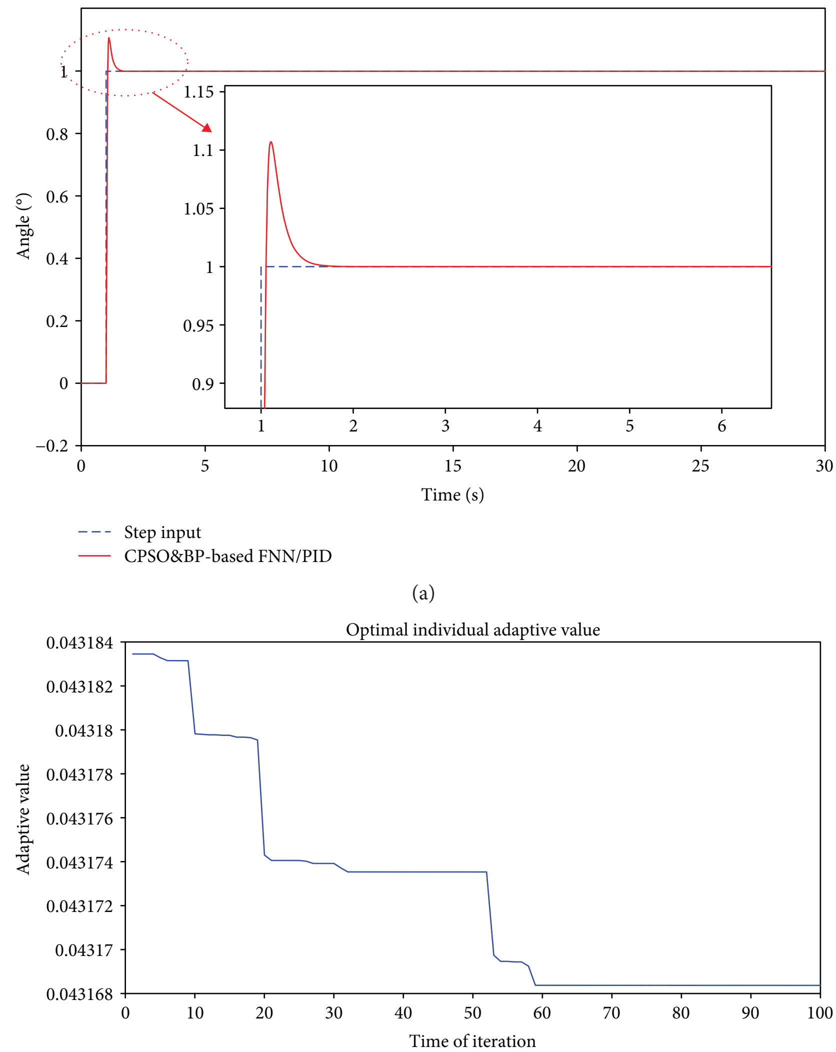

(a)

(b)

Figure 12: Optimal result map of weight coefficient matrix of the FFN/PID controller. (a) Response curve of the FFN/PID control to the step input. (b) Optimization process curve of optimal individual adaptive value.

Table 2: The numerical results on the stabilization precision obtained three different methods responding to the step input.

Control methods	0–30s	Improvement (%) FFN/PID vs. PID	Improvement (%) FFN/PID with optimized parameters vs. FFN/PID with unoptimized parameters
PID/RMS (°)	0.0931	—	—
FFN/PID based on trial and error method/RMS (°)	0.0432	53.6	—
FFN/PID based on composite parameter optimization method/RMS (°)	0.0214	77.0	50.5

disturbance rejection ability. Furthermore, compared with the FFN/PID based on the trial and error method, the FFN/PID based on the composite parameter optimization method is more prominent, by which the stabilization precision is improved up to 50.5% than the former

(3) The CPSO algorithm has strong global search capability, which could escape from local optimizations and approach the global optimizations, by which the FNN/PID compound controller can realize excellent adaptive convergence

Nomenclature

BP: Back propagation
c_1, c_2: Acceleration constants

c, σ:	The centers and widths of activation function
CPSO:	Chaos particle swarm optimization
e:	The error input interface in the FNN/PID control method
Ex, Ey, Ez:	Photoelectric encoders installed on R-gimbal, P-gimbal, and A-gimbal
E_r, E_p, E_a:	Photoelectric encoder measuring relative angular between gimbals
ec:	The error change of input interface in the FNN/PID control method
FNN:	Fuzzy neural network
Gp, Gr, Ga:	Rate gyros measuring the inertial angular rates of P-gimbal, R-gimbal, and A-gimbal
G-pos, G-spe, and G-cur:	The controllers in the position loop, speed loop, and current loop
ISP:	Inertially stabilized platform
PID:	Proportion integration differentiation
J_l:	The moment of inertia of the gimbals along the rotation axis
J_m:	The moment of inertia of the motor
k:	Constant of exponential reaching law representing reaching speed
K_{p0}, K_{i0}, K_{d0}:	The initial parameters of the fuzzy/PID controller
K_t:	The torque coefficient of the motor
k_T:	Torque coefficient of motor
L:	Inductance of torque motor
Mr, Mp, Ma:	Gimbal servo motors of R-gimbal, P-gimbal, and A-gimbal
N:	Transmission ratio
Pos_i:	The position of a particle
R:	Resistance of torque motor
V_i:	The velocity of a particle
w:	Connection weight matrix
w_{all}:	The weight matrix of the BP network
w_p:	Inertia weight
$w_{p\ \max}, w_{p\ \min}$:	The maximum inertia weight and the minimum inertia weight
X_i:	The input variable of Gaussian function and bell-shaped function
μ:	The control parameter of the chaotic motion
α_{co}:	Search radius
λ_{co}:	Iteration times
ω_s:	Critical Stribeck speed.

Data Availability

The data used to support the findings of this study are included in the article.

Conflicts of Interest

The authors declare that there is no conflict of interest regarding the publication of this paper.

Acknowledgments

This project is supported in part by the National Natural Science Foundation of China (Grant nos. 51775017 and 51375036), by the Beijing Natural Science Foundation (Grant no. 3182021), and by the Open Research Fund of the State Key Laboratory for Manufacturing Systems Engineering (sklms2018005).

References

[1] H. Zhang, H. Song, and B. Yu, "Application of hyper spectral remote sensing for urban forestry monitoring in natural disaster zones," in *2011 International Conference on Computer and Management (CAMAN)*, pp. 1–4, Wuhan, China, May 2011.

[2] S. Salahova, "High resolution space images for hazardous waste area monitoring with application of remote sensing and GIS," *International Journal of Aeronautical and Space Sciences*, vol. 9, no. 1, pp. 42–47, 2008.

[3] K. Ahmad, M. Riegler, K. Pogorelov, N. Conci, P. Halvorsen, and F. De Natale, "JORD: a system for collecting information and monitoring natural disasters by linking social media with satellite imagery," in *Proceedings of the 15th International Workshop on Content-Based Multimedia Indexing - CBMI '17*, pp. 1–6, Florence, Italy, June 2017.

[4] Y. Lan, S. J. Thomson, Y. Huang, W. C. Hoffmann, and H. Zhang, "Current status and future directions of precision aerial application for site-specific crop management in the USA," *Computers and Electronics in Agriculture*, vol. 74, no. 1, pp. 34–38, 2010.

[5] G. Cantoro, J. Pelgrom, and T. D. Stek, "Reading a difficult landscape from the air. A methodological case-study from a WWII airfield in South Italy," *Journal of Cultural Heritage*, vol. 23, Supplement, pp. 12–19, 2017.

[6] S. Wang, K. Adhikari, Q. Wang, X. Jin, and H. Li, "Role of environmental variables in the spatial distribution of soil carbon (C), nitrogen (N), and C:N ratio from the northeastern coastal agroecosystems in China," *Ecological Indicators*, vol. 84, pp. 263–272, 2018.

[7] K. T. Sanders and S. F. Masri, "The energy-water agriculture nexus: the past, present and future of holistic resource management via remote sensing technologies," *Journal of Cleaner Production*, vol. 117, pp. 73–88, 2016.

[8] J. M. Hilkert, "Inertially stabilized platform technology concepts and principles," *IEEE Control Systems*, vol. 28, no. 1, pp. 26–46, 2008.

[9] X. Zhou, H. Zhang, and R. Yu, "Decoupling control for two-axis inertially stabilized platform based on an inverse system and internal model control," *Mechatronics*, vol. 24, no. 8, pp. 1203–1213, 2014.

[10] J. M. Hilkert, "Adaptive control system techniques applied to inertial stabilization systems," in *Proceedings Volume 1304, Acquisition, Tracking, and Pointing IV*, pp. 190–206, Orlando, FL, USA, September 1990.

[11] P. J. Kennedy and R. L. Kennedy, "Direct versus indirect line of sight (LOS) stabilization," *IEEE Transactions on Control Systems Technology*, vol. 11, no. 1, pp. 3–15, 2003.

[12] X. Zhou, B. Zhao, W. Liu, H. Yue, R. Yu, and Y. Zhao, "A compound scheme on parameters identification and adaptive compensation of nonlinear friction disturbance for the aerial inertially stabilized platform," *ISA Transactions*, vol. 67, no. 3, pp. 293–305, 2017.

[13] M. K. Masten, "Inertially stabilized platforms for optical imaging systems," *IEEE Control Systems Magazine*, vol. 28, no. 1, pp. 47–64, 2008.

[14] X. Zhou, Y. Jia, Q. Zhao, and T. Cai, "Dual-rate-loop control based on disturbance observer of angular acceleration for a three-axis aerial inertially stabilized platform," *ISA Transactions*, vol. 63, no. 7, pp. 288–298, 2016.

[15] K. Deng, F. Long, and S. Wang, "Simulating optimal control of an inertial platform stabilization loop using genetic algorithms," in *2013 Fourth Global Congress on Intelligent Systems*, pp. 177–181, Hong Kong, China, December 2013.

[16] G. Sun, X. Wu, and Z. Zhong, "A self-tuning fuzzy-PID stabilization experiment of a seeker inertial platform's tracking loop subject to input saturation and dead-zone," in *2016 IEEE International Conference on Aircraft Utility Systems (AUS)*, pp. 580–585, Beijing, China, October 2016.

[17] Y. Huang, H. Cai, and X. Bai, "Research on stability control of floated inertial platform based on ADRC," in *Proceedings Volume 10244, International Conference on Optoelectronics and Microelectronics Technology and Application*, Shanghai, China, January 2017.

[18] F. Wang, D. Tian, and Y. Wang, "High accuracy inertial stabilization via Kalman filter based disturbance observer," in *2016 IEEE International Conference on Mechatronics and Automation*, pp. 794–802, Harbin, China, August 2016.

[19] Y. Yang, H. Li, P. Jia, and Y. Wang, "RISE-based tracking control of inertial stabilized platform with extended disturbance observer," in *2016 12th IEEE International Conference on Control and Automation (ICCA)*, pp. 632–637, Kathmandu, Nepal, June 2016.

[20] M. Li, J. Li, and R. Zhang, "Unbalance disturbance restraining for inertial stabilized platform," in *2016 Chinese Control and Decision Conference (CCDC)*, pp. 2723–2728, Yinchuan, China, August 2016.

[21] Z. Yu, J. Z. Cao, H. T. Yang, H. N. Guo, B. Gao, and L. Yang, "Advanced fuzzy PID composite control for stabilized platform system," in *2012 IEEE International Conference on Mechatronics and Automation*, pp. 2536–2540, Chengdu, China, August 2012.

[22] H. Wang and Y. Bao, "Fuzzy-PID dual mode fuzzy control of the electro-hydraulic deviation control system," in *2010 International Conference on Mechanic Automation and Control Engineering*, pp. 3137–3140, Wuhan, China, June 2010.

[23] W. W. Chen, Y. K. Liu, X. Y. Tan et al., "PID parameter optimization based on fuzzy control," *Advanced Materials Research*, vol. 960-961, pp. 1156–1161, 2014.

[24] W. Cao and Q. Meng, "Based on PLC temperature PID - fuzzy control system design and simulation," in *2010 International Conference on Information, Networking and Automation (ICINA)*, pp. 417–421, Kunming, China, October 2010.

[25] W. He and Y. Dong, "Adaptive fuzzy neural network control for a constrained robot using impedance learning," *IEEE Transactions on Neural Networks and Learning Systems*, vol. 29, no. 4, pp. 1174–1186, 2018.

[26] H. Qiu, "The reserch of variable structure fuzzy neural network control system," in *2016 IEEE International Conference of Online Analysis and Computing Science (ICOACS)*, pp. 273–276, Chongqing, China, May 2016.

[27] S. Binitha and S. Sathya, "A survey of bio inspired optimization algorithm," *International Journal of Soft Computing & Engineering*, vol. 2, no. 2, pp. 137–151, 2012.

[28] B. Borowska, "An improved CPSO algorithm," in *2016 XIth International Scientific and Technical Conference Computer Sciences and Information Technologies (CSIT)*, pp. 1–3, Lviv, Ukraine, September 2016.

[29] I. Ziari and A. Jalilian, "A PSO-based approach to adjust CPSO parameters," in *Proceedings of 14th International Conference on Harmonics and Quality of Power - ICHQP 2010*, pp. 1–6, Bergamo, Italy, September 2010.

[30] J. Tao, Q. Sun, S. Luo, W. Liang, and Z. Chen, "CPSO based optimization in multiphase homing trajectory of powered parafoils with insufficient altitude," in *2016 35th Chinese Control Conference (CCC)*, pp. 5386–5391, Chengdu, China, July 2016.

[31] A. Mahmoudabadi and A. Ghazizadeh, "A hybrid PSO-fuzzy model for determining the category of 85th speed," *Journal of Optimization*, vol. 2013, Article ID 964262, 8 pages, 2013.

[32] W. Liu, N. Luo, G. Pan, and A. Ouyang, "Chaos particle swarm optimization algorithm for optimization problems," *International Journal of Pattern Recognition and Artificial Intelligence*, vol. 32, no. 11, p. 1859019, 2018.

[33] L. Mengxia, L. Ruiquan, and D. Yong, "The particle swarm optimization algorithm with adaptive chaos perturbation," *International Journal of Computers Communications & Control*, vol. 11, no. 6, pp. 804–818, 2016.

[34] H. Zhao, Z. Ru, X. Chang, and S. Li, "Reliability analysis using chaotic particle swarm optimization," *Quality and Reliability Engineering International*, vol. 31, no. 8, pp. 1537–1552, 2014.

[35] D. K. Sambariya and R. Prasad, "Selection of membership functions based on fuzzy rules to design an efficient power system stabilizer," *International Journal of Fuzzy Systems*, vol. 19, no. 3, pp. 813–828, 2016.

[36] Y. Zhang and H. Lv, "Study on PID controller based on fuzzy RBF neural network in rolling mill hydraulic AGC system," in *2016 Chinese Control and Decision Conference (CCDC)*, pp. 4616–4620, Yinchuan, China, May 2016.

[37] J. Gou, W. P. Guo, C. Wang, and W. Luo, "A multi-strategy improved particle swarm optimization algorithm and its application to identifying uncorrelated multi-source load in the frequency domain," *Neural Computing and Applications*, vol. 28, no. 7, pp. 1635–1656, 2016.

[38] H. Liu, M. Huang, and D. Huang, "Survey on optimization method based on chaotic search and its developments," *Journal of Nanjing University of Science and Technology*, vol. 29, no. 144, pp. 124–128, 2005.

[39] X. Xu, H. Rong, M. Trovati, M. Liptrott, and N. Bessis, "CS-PSO: chaotic particle swarm optimization algorithm for solving combinatorial optimization problems," *Soft Computing*, vol. 22, no. 3, pp. 783–795, 2016.

[40] H. Xing, B. Hou, Z. Lin, and M. Guo, "Modeling and compensation of random drift of MEMS gyroscopes based on least squares support vector machine optimized by chaotic particle swarm optimization," *Sensors*, vol. 17, no. 10, article 2335, 2017.

[41] J. Liu and X. Han, "Application of CPSO optimizing NN arithmetic on nonlinear dynamic system," in *2009 International*

Conference on Information Engineering and Computer Science, Wuhan, China, December 2009.

[42] G. A. Santana, F. R. Durand, and T. Abrão, "Power allocation in PON-OCDMA with improved chaos particle swarm optimization," *Journal of Microwaves, Optoelectronics and Electromagnetic Applications*, vol. 17, no. 2, pp. 268–283, 2018.

[43] J. J. Yao, Q. T. Niu, T. Wang et al., "Acceleration harmonic identification for an electro-hydraulic shaking table based on BP network," in *2016 Chinese Control and Decision Conference (CCDC)*, pp. 3328–3332, Yinchuan, China, May 2016.

[44] X. Zhou, B. Zhao, and G. Gong, "Control parameters optimization based on co-simulation of a mechatronic system for an UA-based two-axis inertially stabilized platform," *Sensors*, vol. 15, no. 8, pp. 20169–20192, 2015.